

Lasers in Manufacturing Conference 2021

Investigation of Kovar in PBF-LB/M

Arvid Abel^{a, 1}, Jakob Pufal^a, Vitaly Rymanov^b, Christian Hoff^a, Jörg Hermsdorf^a,
Sumer Maklouf^c, Jörg Lackmann^c, Andreas Stöhr^{b,c}, Stefan Kaierle^a

^aLaser Zentrum Hannover, Hollerithallee 8, Hannover, 30419, Germany

^bMicrowave Photonics GmbH, Essener Straße 5, Oberhausen, 46047, Germany

^cUniversität Duisburg-Essen, Zentrum für Halbleitertechnik und Optoelektronik, Lotharstraße 55, Duisburg, 47057, Germany

Abstract

The iron-nickel-cobalt alloy Kovar is highly desirable in glass-to-metal hybrid components, e.g., hermetic seals, or as packaging material in high-frequency microsystems due to its thermal expansion coefficient similar to borosilicate glass. Hitherto, the processability of Kovar in additive manufacturing has only been insufficiently investigated, leaving the potential of this material for functional integrated components unused. This paper describes the processing in PBF-LB/M and the understanding of the process parameters to achieve a relative density over 99.9 % in test specimens, large volumes, and complex structures. The investigated factors were laser power, scanning speed, and hatch distance. The initial experiments were done as full factorial designs. Subsequent investigations were done within the design of experiments to develop an empirical process model for the fabrication of Kovar in the PBF-LB/M. The best results were fabricated with volumetric energy densities between 200 to 350 to achieve a maximum density of 99.96 %.

Keywords: Powder Bed Fusion by Laser Beam; Kovar; Additive Manufacturing; Design of Experiments; Additive Processing

1. Introduction

Photonic millimeter-wave generation using Radio-over-Fiber (RoF) systems is of great importance for many emerging markets as it provides ultrawide tunability, broadband modulation, and enables the utilisation of low-loss fiber-optical signal transport. Applications, such as wireless backhauling, spectroscopy, imaging, and sensing, or the medical sector, are utilizing innovative and custom-designed RoF components and systems operating in the micro- and millimeter-wave bands (Stöhr, 2010; Ahmed et al., 2011; Tseng et al., 2013; Seeds

* Corresponding author. Tel.: +49 511 2788 482; fax: +49 511 2788 100.
E-mail address: A.Abel@lzh.de.

et al, 2015). For packaging the chips, interfaces, waveguides and connectors, additive manufacturing can be very beneficial, since the variety of applications often requires the manufacturing of customized RoF packages.

For fabricating these packages, the power bed fusion by laser beam (PBF-LB/M) can manufacture the parts with a high degree of complexity und functionalization, resulting in more design options, compact parts and cost efficiency. The PBF-LB is a process in which the desired part geometry is created by fusing layers on top of each other, generating the geometry additively in a metal powder bed (Lachmayer et al., 2016). The iron-nickel-cobalt alloy Kovar as a material for the package is highly desirable due to the similar thermal expansion coefficient compared to indium phosphide, which is the preferred material for the optical chips such as lasers, photodiodes and RF electronics. Kovar enables the development of temperature-insensitive RoF packages that do not require active cooling (Castillo et al., 2011; Ulrich et al., 2015) So far, the processability of Kovar in additive manufacturing has been insufficiently investigated. In this study, process knowledge of Kovar in the PBF-LB is generated. The influence of different parameters on the density is investigated. The aim is to produce large and small geometries as well as test specimen for thin walls with a relative density of more than 99.9 %.

2. Materials and Methods

2.1. Machine set up and materials

The machine setup used in this investigation is the PBF-LB system TruPrint 1000 by Trumpf GmbH + Co. KG (Ditzingen, Germany). The system is equipped with a 1070 nm continuous wave ytterbium fiber laser with an energy output of 200 W and laser spot diameter of 30 μm . The investigated Kovar alloy was supplied by Sandvik AB (Stockholm, Sweden). The particle diameters ranging from 15 to 53 microns and are shown in the figure 1.

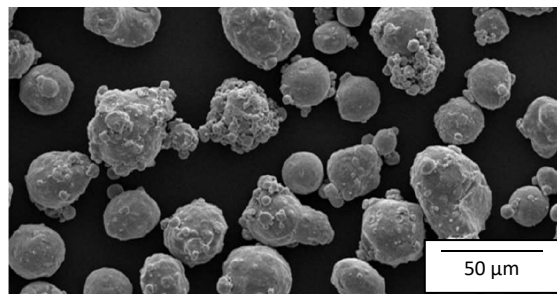


Fig. 1. SEM Image of Kovar particles

The evaluation of the build specimen regarding the density is achieved by analyzing microscopic images of cross sections with a VK-X1000 by Keyence (Neu-Isenburg, Germany). For this purpose, the specimen are embedded in an epoxy resin and grinded as well as polished with a Tegramin-30 by Stuers (Ballerup, Denmark).

2.2. Methods

This paper describes the methods of processing a novel material in the PBF-LB, starting without preliminary experiences and delivering an empirical process model to have a deep understanding of the melting process. The processing will be optimized on cubes with 5 mm edge length and validated with thin walls (2 – 0.5 mm) and bigger cubes (15 x 10 x 8 mm) for complex structures and larger applications. These specimen shall investigate the expected change in optimal energy input due to different heat transfer rates. Especially in thin

walls it is expected, that the reduction in heat transfer can lead to remaining porosity of the build structures induced by evaporations of the melt.

Along the process of optimizing the relative density of the fabricated specimen in this investigation, an empirical process model is set up to guide shifts in parameters to minimize excess trials to get to the target of 99.9 % relative density. This predictive process model is generated with the software JMP (SAS Institute, Heidelberg, Germany) and links the input variables (fabrication parameters) as a Taylor polynomial of second degree to the output variables (relative density) with the method of least squares. The input variables and their connections are investigated for their significance i.e. sensitivity on the output variable and the influence of the parameters can be predicted.

The quality of this regression can be evaluated by the deviation of prediction to the as build specimen. In this study, the regression coefficient R^2 and the root mean square error (RMSE) are used to evaluate the accuracy of the model. Although the R^2 -value does not have a clear cut-off above which a good correlation exists, the value indicates a good correlation, when the value is closer to 1 than to 0. The RMSE shows the averaged deviation between the density of the prediction and the as build specimen. There are no target values for R^2 and the RMSE, as they are used to judge the fit of the model. The investigated parameters for the processing of Kovar are adopted from stainless steel (1.4404) due to similarities in alloy composition, phase transition temperatures and heat transfer rates. These used parameters are laser power, scanning speed and hatch distance.

2.3. Experimental set up

In this investigation, four trials were accomplished. Since the feasibility of processing Kovar in the PBF-LB must first be demonstrated, the first experiment serves as a starting point for further processing. In order to minimize the influential factors on the process, the specimen will be melted on the substrate. This reduces irregularities in the process induced by changing heat transfer in support structures. The second investigation transfers the knowledge about the processing parameters to test specimens with support structures. After the attainment of the parameter interval to process dense specimen with and without support structure, these parameters have to be validated or further optimized in the third experiment. In the final investigation, the geometry of the specimen will be altered for larger or complex applications, resulting in separate optimal parameters for each geometrical boundary condition. The investigated parameters are in the table 1 below. All investigations were carried out as full factorial designs, because the first experiment already accomplished the desired target density as a starting point. This experiment was set up to establish an empirical process model to guide the shifts in parameters in the full factorial designs through this investigation. Only minor adjustments to the parameters were necessary, therefore, a change in experimental design was not expedient.

Table 1. Parameters of the investigation

Process parameter (Number of Steps)	Trial 1: Cubes without support structure	Trial 2: Cubes with support structure	Trial 3: Validation on cubes	Trial 4: Validation on large / thin structure
Laser power [W]	100 – 160 (4)	160 – 170 (3)	150 – 170 (5)	160 – 170 (3)
Scanning speed $\left[\frac{\text{mm}}{\text{s}}\right]$	400 – 1000 (4)	400 – 800 (5)	500 – 700 (5)	300 – 500 (3)
Hatch distance [μm]	40 – 80 (3)	40 – 80 (3)	80 (1)	80 (1)

3. Experimental results

3.1. First experiment – cubes without support structure

As described in the previous chapter, the study was divided into four experiments, with a total of 166 build and analysed specimen. The first experiment was intended as a starting point for further refinement of the parameter interval. The results of the first experiment are shown in the figure 2 below. The figures on the left displaying the relative densities of the parameters. The green highlighted results show the parameter set with rel. densities over or equal 99.9 %. The image on the right is a cross section of the best result.

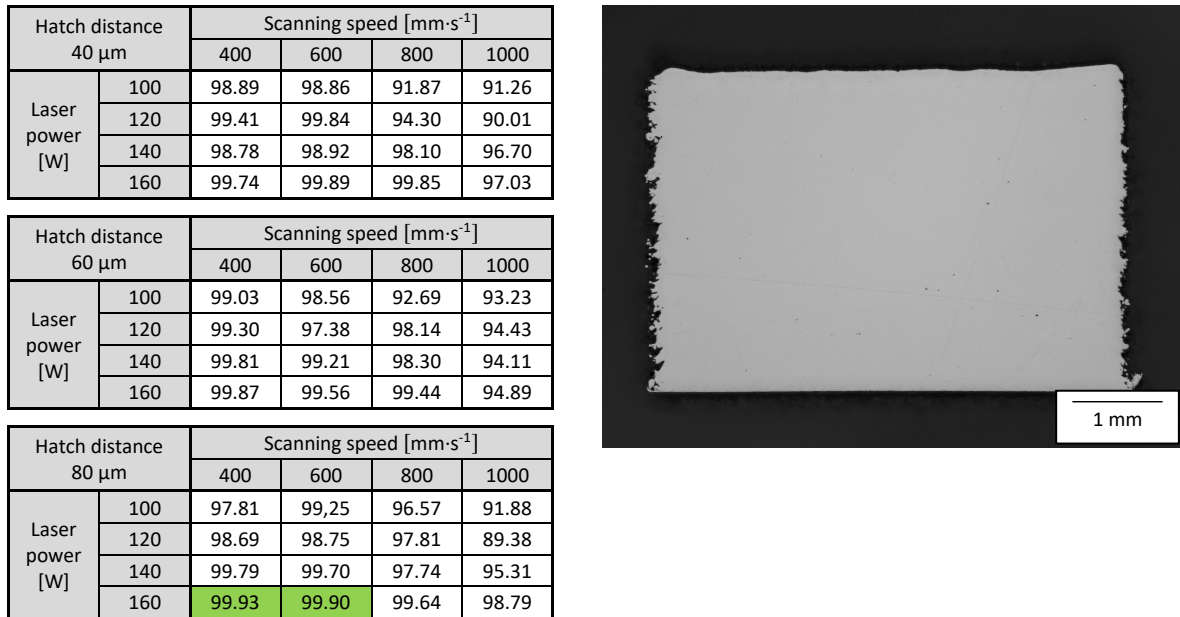


Fig. 2. Results of the first experiment. Left: Relative densities. Right: Cross section of the best result with a density of 99.93 %

The results show, that the processability of Kovar in the PBF-LB could be approved and a starting point for further investigation was set. To get a statistical assessment of the optimal processing window an empirical process model of the first experiment was set up. Using the software JMP, the prediction model resulted in a regression coefficient of $R^2 = 0.81$ with a root mean square error (RMSE) of 1.36 %. These values are considered for the further investigations as a basis for comparison. Within the parameter boundaries of the first experiment, this model suspects the highest density at 160 W, 600 mm/s and 80 μm . Although this is only the second best parameter, a relative density over 99.9 % can be achieved with this parameter. It can be assumed, that the model has slight deviations, but reflects the optimal processing window. The figure 3 displayed the prediction graphs of the input variables. With the above mentioned parameters a density of 100.48 is predicted, which is not technically possible, but due to approximation errors of this model.

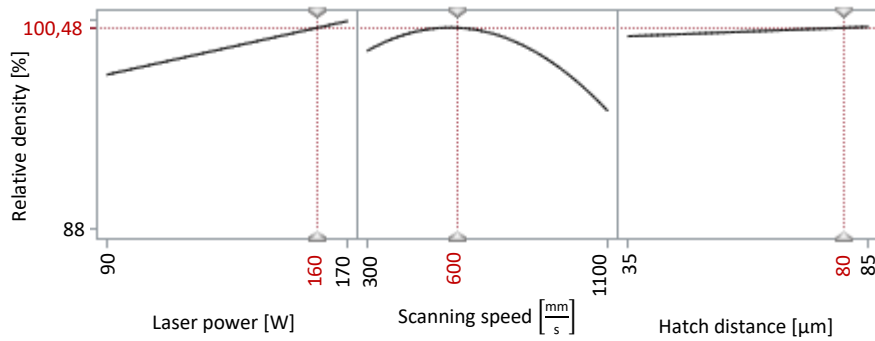


Fig. 3. Prediction graphs of first empirical model

The prediction of the empirical model shows that the density could be further improved by increasing the laser power. The scanning speed is close to the maximum and has to be investigated in more detail. The hatch distance shows no significant influence.

3.2. Second experiment

The aim of the second investigation was to investigate the influence of a 3 mm support structure on the melting process. It is expected, that a slight shift in the optimal processing parameter will occur, due to the impairment of the heat transfer through the support structure. The figure 4 displays the results.

Hatch distance 40 μm		Scanning speed [$\text{mm}\cdot\text{s}^{-1}$]					
		300	400	500	600	700	800
Laser power [W]	160		98.68	99.72	98.41	99.84	99.10
	165		99.82	99.42	99.90	92.15	95.44
	170	88.32	98.97	99.86	90.32	90.66	96.13

Hatch distance 60 μm		Scanning speed [$\text{mm}\cdot\text{s}^{-1}$]					
		300	400	500	600	700	800
Laser power [W]	160		95.42	99.54	98.91	99.89	99.89
	165		98.65	99.09	98.56	99.86	93.49
	170	95.99	98.86	99.22	99.66	93.14	95.06

Hatch distance 80 μm		Scanning speed [$\text{mm}\cdot\text{s}^{-1}$]					
		300	400	500	600	700	800
Laser power [W]	160		95.15	94.75	97.15	98.86	99.88
	165		99.93	99.44	99.18	99.89	99.81
	170	98.77	95.93	98.36	98.29	99.66	87.08

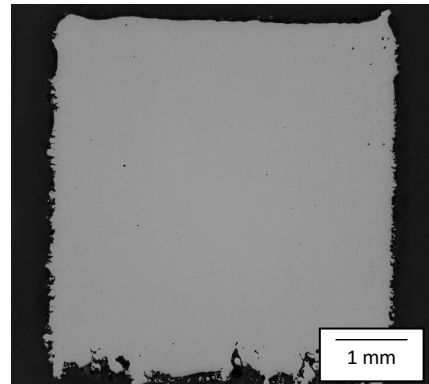


Fig. 4. Results of the second experiment. Left: Relative densities. Right: Cross section of the best result with a density of 99.93 %

There were two parameters, which lead to specimen with relative density above 99.9 %. The best parameters of the first experiment did not yield the best result on the support structures. Nevertheless, the best parameter of this experiment did only differ slightly in laser power from the best result of the first experiment. As seen before, the hatch distance seems to have no significant impact on the density.

The statistical evaluation of this investigation showed a lesser significant fit with an R^2 of 0.41 and an RMSE of 2.872. This confirms the assumption that the change in the heat dissipation of the melt through the support structure has an influence and leads here to a more complex process, which cannot be described as accurately as the first attempt by this empirical model. Since the targets of the relative density have already been met, the process must be checked for repeatability. In addition, further data can extend the empirical model and provide a more precise prediction for subsequent investigations.

3.3. Third experiment – Validation of 1st and 2nd experiment

The third investigation consists of confirming the empirical model of the first experiment on the one hand and the best results of the second investigation on the other hand. Since the empirical model describes the first experiment very well, the best parameters of the first experiment are not repeated exactly but the assumed optimal process window is to be confirmed. Because of the insignificance of the hatch distance in the previous trials it is set to 80 μm , allowing the laser power and scanning step to be investigated in more detail. With these parameters, 25 cubes are built with and without support structure. Moreover, the two best results of the second experiment will be repeated separately. The results are displayed in figure 5.

Without support		Scanning speed [$\text{mm}\cdot\text{s}^{-1}$]				
		500	550	600	650	700
Laser power [W]	150	99.35	99.96	99.92	99.84	99.22
	155	99.95	99.93	99.76	99.31	99.19
	160	99.91	99.92	99.47	98.83	99.38
	165	99.81	99.94	99.77	99.79	99.57
	170	99.85	99.90	99.74	99.59	99.66

With support		Scanning speed [$\text{mm}\cdot\text{s}^{-1}$]				
		500	550	600	650	700
Laser power [W]	150	99.87	95.73	99.03	98.50	96.44
	155	99.60	99.52	99.89	99.55	98.84
	160	99.70	99.88	99.29	99.44	94.16
	165	99.80	99.82	99.60	98.51	97.05
	170	98.64	99.87	99.76	99.21	98.91

Addition	#	Power	Speed	Hatch	Support	Density
	1	165	600	40	yes	99.89
	2	165	400	80	yes	99.92

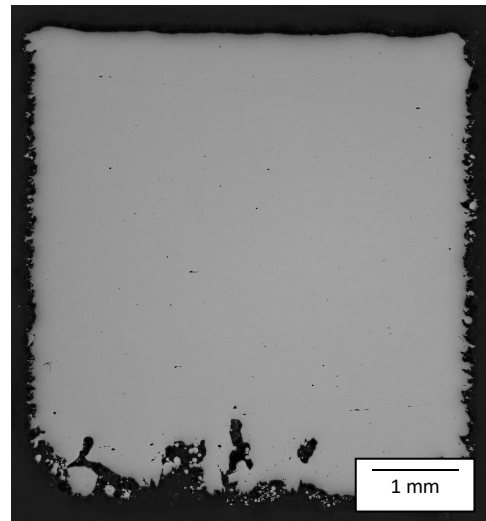


Fig. 5. Results of the third experiment. Left: Relative densities in data table. Specimen with a density over 99.9 % highlighted green. Right: Image of cross section of the best result with support with a density of 99.92 %

This parameter interval did not provide good results for the cubes with support structures, showing that the processing interval of the empirical model is only suitable for processing cubes without support structures. Although no good results could be generated in this new parameter window with support structures, the best results of the second experiment were confirmed and provided the best results again here. Due to these results, it is suspected that the process is repeatable.

Due to the wide range of very good results for cubes without support structures, the prediction model can be confirmed. The recommended parameter is 160 W, 550 mm/s and 80 μm . This parameter is between the best results of the first experiment and the centre of the best parameters of the third experiment. The prediction formula can be extracted and used for a contour plot of the relative density. This plot is displayed in figure 6. The graph shows the contour lines of areas with predicted relative densities in relation to the fabrication parameters. The dots are the results with fabricated densities over 99.9 %. It is evident, that the prediction has deviations. Therefore, the model can only be used with the RMSE of 1.13 % as a tolerance.

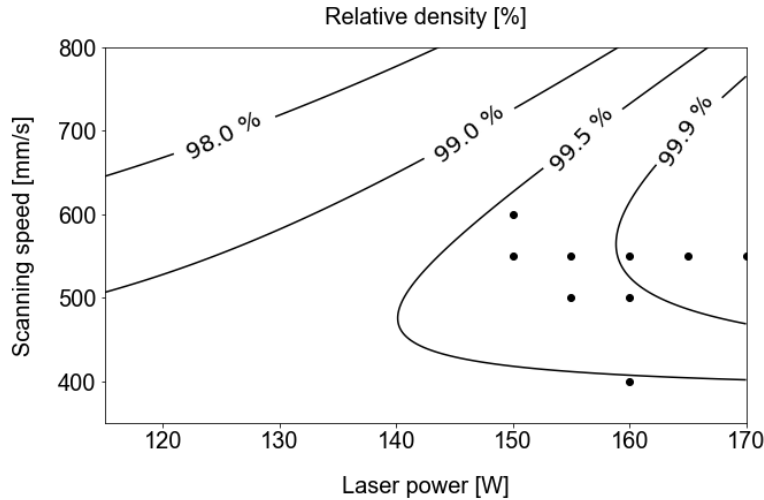


Fig. 6. Contour plot of Kovar fabrication

3.4. Fourth experiment – Validation on larger and smaller volumes

After finishing the research on the parameters for the small cubes, the influence of different geometry must now be investigated. Because the investigations with support structures have reacted more sensitively on the input variables, it is expected that with the control of this process behavior the results are just as valid for the less sensitive process without support. Therefore, only the parameters for the support structure are investigated. The center of the parameter interval is the best parameter of the second and third experiment. It is expected to deliver the same results in bigger structures and have a lower limit for the smaller structures. In thin walls it is common to adjust the parameters for less energy input due to the decreased heat transfer. The results are displayed in figure 7. The following table shows the results of the examination of the large cubes and the densities achieved in the walls with different wall thicknesses.

It can be seen, that there were four parameter combinations that resulted in relative densities above 99.9 % in the large cubes. Here, the best result of the second and third experiment could be confirmed. It is evident, that there is no parameter, which leads to the target density in all wall thicknesses. The assumption can be confirmed that a slight reduction of the energy input is necessary with decreasing wall thicknesses.

#	Input		Relative density [%]					
	Laser power [W]	Scanning speed [mm·s ⁻¹]	Larger cube	Thin structure with wall thickness:				
				2 mm	1.5 mm	1 mm	0.75 mm	0.5 mm
1	160	300	99,54	98,31	98,25	98,14	98,07	99,93
2	160	400	99,95	99,94	99,79	98,89	98,49	97,22
3	160	500	99,85	99,86	99,84	99,91	99,90	99,91
4	165	300	99,78	99,63	99,82	99,75	99,77	99,93
5	165	400	99,92	99,67	99,67	99,46	99,52	99,97
6	165	500	99,90	99,84	99,85	99,50	98,80	99,90
7	170	300	99,90	99,92	99,46	97,47	96,39	95,19
8	170	400	99,66	99,85	99,78	99,58	99,31	97,99
9	170	500	98,94	99,86	99,88	99,93	99,95	99,85

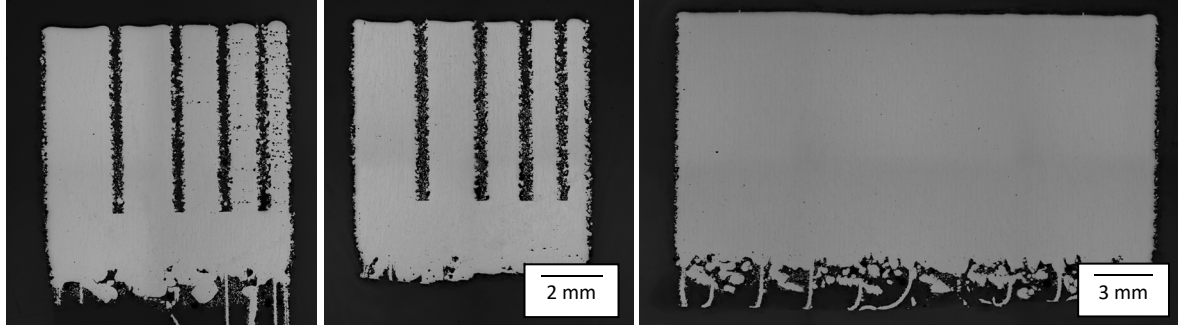


Fig. 7. Results of fourth experiment. Specimen with a density over 99.9 % highlighted green. Displayed specimen (left to right): suboptimal parameter for thin walls (#7), optimal parameter (#3) and validated parameter for large structure (#5).

Thus, the best parameter (#5, 165 W , 400 mm/s) of the previous tests is valid for cubes with 5 mm edge length, but better results are already obtained for the 2 mm walls when the power is reduced by five watts (shift to parameter #2). If the wall thicknesses are reduced even more, this parameter must be adjusted further and the reduction of the energy input can be achieved here by increasing the scanning speed (shift to parameter #3). Thus, all wall thicknesses can be built up well. Although the value of 99.9 % relative density was target in this study, the result of the relative density of parameter #3 with 99.86 and 99.84 for wall thicknesses of 2 mm and 1.5 mm is sufficient as seen in the cross section of the walls in the lower centre of figure 7.

4. Conclusion

This paper shows the feasibility of the processing of Kovar in the PBF-LB/M. Several process parameter sets lead to specimen with relative densities above 99.9 % and could be repeated with and without support structure as well as in large structures and thin walls. The influence of different geometries on the process could be shown and a change in optimal process parameters was stated. Further investigation could determine the material properties. In addition, the use as a material in the aforementioned RoF packages is conceivable. Another area that Kovar opens up is hybrid processing with glass to produce a material bond or vacuum tight assemblies.

References

- Ahmed, Schiessl, Schmidt. 2011. A novel fully electronic active real-time imager based on a planar multistatic sparse array. *IEEE Trans. Microw. Theory Tech.* 59. 3567–3576.
- Castillo, Hoffman, Birur. 2011. Advanced housing materials for extreme space applications. *Aerospace Conference*. pp. 1-6. doi: 10.1109/AERO.2011.5747467.
- Lachmayer, Lippert, Fahlbusch. 2016. *3D Druck beleuchtet*. Springer. Berlin. ISBN 978-3-662-49056-3.
- Seeds, Shams, Fice, Renaud. 2015. Terahertz photonics for wireless communications. *J. Lightwave Technol.* 33. 579–587.
- Stöhr. 2010. Photonic millimeter-wave generation and its applications in high data rate wireless access. In *Proceedings of the IEEE International Topical Meeting on Microwave Photonics*. Montreal, QC, Canada. pp. 7–10.
- Tseng, Wun, Chen, Peng, Shi, Sun. 2013. High-depth-resolution 3-dimensional radar-imaging system based on a few-cycle W-band photonic millimeter-wave pulse generator. *Opt. Express*. 21. 14109–14119.
- Ulrich, Fischer-Hirschert. 2015. *Photonic Packaging Sourcebook: Fiber-Chip Coupling for Optical Components, Basic Calculations, Modules*. Springer. ISBN 3642253768, 9783642253768.